ОБЪЕДИНЕННЫЙ
ИНСТИТУТ
ЯДЕРНЫХ
ИССЛЕДОВАНИЙ

Дубна

E2 - 5216

O.V. Dumbrais, T.Yu. Dumbrais
N.M. Queen

A THEORETICAL MODEL-INDEPENDENT DETERMINATION OF THE REAL PARTS OF THE $K^{\pm}p$ FORWARD SCATTERING AMPLITUDES

ЛАБОРАТОРИЯ ТЕОРЕТИЧЕСКОЙ ФИЗИКИ
ЛАБОРАТОРИЯ ВЫСОКИХ ЭНЕРГИЙ

1970

E2 - 5216

O.V. Dumbrais, T.Yu. Dumbrais[x]
N.M. Queen[xx]

A THEORETICAL MODEL-INDEPENDENT DETERMINATION OF THE REAL PARTS OF THE $K^{\pm}p$ FORWARD SCATTERING AMPLITUDES

Submitted to Nuclear Physics

[x] Institute of Theoretical Physics, Kiev
[xx] On leave of absence from the University of Birmingham, England.

Summary

A new method of analyzing the experimental data on kaon-proton scattering is used to obtain an accurate determination of the real parts of the forward scattering amplitudes at moderate energies.

The method exploits the known analyticity properties of the scattering amplitude and experimental data in a limited energy range However, unlike conventional dispersion relation calculations, it requires no assumptions about the residues of the hyperon pole terms and the amplitudes in the unphysical and asymptotic regions. A parameter describing the unknown asymptotic behaviour of the difference of the K^-p and K^+p total cross sections is determined. Its value favours a zero asymptotic limit for this difference but requires a slower approach to zero than that predicted by conventional Regge pole models which satisfy the Pomeranchuk theorem. The method can be used in principle to analytically continue the scattering amplitude from the physical region to the Λ pole. However, a sufficiently accurate model-independent determination of the $KN\Lambda$ coupling constant cannot be obtained in this way using the experimental data which exist at the present time.

1. Introduction

The real parts of the $K^{\pm}p$ forward scattering amplitudes have been predicted independently by many authors[1-6], in terms of the experimentally known total cross sections according to a variety of dispersion relations. The motivations for such calculations are well known[7] and will not be discussed here in detail.

Although the results of these calculations are generally in qualitative agreement with each other and with most of the experimental data, there are some significant discrepancies in their detailed structure, especially at energies of the order of a GeV (see, e.g., fig. 28 of ref.[5]). These discrepancies are mainly due to differences in the input data which are used, namely the set of experimental total cross section data, the models used to extrapolate the imaginary parts of the scattering amplitudes into the unphysical and asymptotic regions, and the values of the $KN\Lambda$ and $KN\Sigma$ coupling constants.

The importance of using a method which is not too sensitive to the poorly known coupling constants and to the structure of the $K^{-}p$ amplitude in the unphysical region below the elastic threshold has recently been stressed[4,6]. Nevertheless, all previous calculations, including those of refs.[4,6], have adopted specific parametrizations for the analytic continuation of the scattering amplitude into the unphysical region. This analytic continuation is found to be rather unstable in practice, so that the structure of the amplitude in the unphysical region and hence also the corresponding predictions for the coupling constants (obtained by means of forward dispersion relations) are very sensitive to the parametrization which is chosen[7].

All previous methods of calculating the real parts of the $K^{\pm}p$ forward scattering amplitudes, with one exception[6], have also required the assumption of some specific Regge model for the amplitudes at asymptotic energies. The results of such analyses are now subject to an additional uncertainty, since recent measurements of the K^-p total cross section between 20 and 55 GeV at Serpukhov[8] are in poor agreement with the extrapolations of most earlier simple Regge pole fits to the data at lower energies. Although attempts to fit the new data have been made[9-14], considerable ambiguity remains in the more sophisticated parametrizations, especially those including Regge cuts, so that there is a large uncertainly in the extrapolation of the amplitudes to higher energies.

The new Serpukhov data[8] have in fact raised serious doubts about the validity of the Pomeranchuk theorem for $K^{\pm}p$ scattering. If the Pomeranchuk theorem is violated, most of the conventional methods of calculating the real parts of the forward scattering amplitudes, based on dispersion relations with only one subtraction, would be invalid in principle. On the other hand, it has been noticed[7,15] that numerical calculations based on the standard dispersion relations with two subtractions[2] involve unpleasantly strong cancellations among the various low-energy contributions.

In the present paper we re-analyze all the available experimental data on the real and imaginary parts of the $K^{\pm}p$ forward scattering amplitudes by means of a new method which avoids the difficulties mentioned above. In this way we obtain a model-independent theoretical fit to the real parts of the amplitudes at moderate energies. Unlike all previous analyses, our method requires as input information only experimental data on the real and imaginary parts of the amplitudes in a finite interval of the physical region. No assumptions are required about the Λ and Σ poles and the amplitudes on the unphysical cut and in the asymptotic region.

2. The Discrepancy Function

We denote by $f_{\pm}(\omega) = D_{\pm}(\omega) + i\,A_{\pm}(\omega)$ the forward $K^{\pm}p$ scattering amplitudes in the laboratory frame, normalized so that the optical theorem takes the form

$$\sigma_{\pm}(\omega) = 4\pi A_{\pm}(\omega)/k, \tag{1}$$

where k and ω are the laboratory momentum and energy of the kaon respectively.

We now define the function

$$\Delta(\omega) = D_{-}(\omega) - D_{+}(m_K) + \frac{\omega + m_K}{\pi}\,[I(\omega) + J(\omega)], \tag{2}$$

where

$$I(\omega) = (4\pi)^{-1}\, P\int_{m_K}^{W} \left[\frac{\sigma_{+}(\omega')}{(\omega' - m_K)(\omega' + \omega)} - \frac{\sigma_{-}(\omega')}{(\omega' + m_K)(\omega' - \omega)}\right] k'\,d\omega', \tag{3}$$

$$J(\omega) = -\,\mathrm{Im} \int_{S(W)} \frac{f_-(\omega')\,d\omega'}{(\omega' + m_K)(\omega' - \omega)}. \tag{4}$$

Here W is the highest energy at which the total cross sections $\sigma_{\pm}(\omega)$ are known experimentally, and $S(W)$ denotes the semicircle in the upper half of the complex ω plane given by $|\omega| = W$.

Consider the closed contour in the ω plane consisting of the straight line joining the points $-W + i\epsilon$ and $W + i\epsilon$ $(\epsilon \to 0^+)$ and the semicircle $S(W)$. By applying Cauchy's theorem to the function

$$F(\omega';\omega) = -\frac{f_-(\omega')}{(\omega' + m_K)(\omega' - \omega)} \tag{5}$$

around this contour and using the well known analyticity and crossing properties of $f_{\pm}(\omega)$ /7/, it is straightforward to show that

$$\Delta(\omega) = \frac{\omega + m_K}{\pi}\left[\sum_{Y=\Lambda,\Sigma} \frac{\pi X(Y)}{(\omega_Y + m_K)(\omega_Y - \omega)} + \int_{\omega_{\pi\Lambda}}^{m_K} \frac{A_-(\omega')\,d\omega'}{(\omega' + m_K)(\omega' - \omega)}\right], \tag{6}$$

where

$$\omega_Y = \frac{m_Y^2 - m_p^2 - m_K^2}{2 m_p},$$

$$X(Y) = \frac{g_Y^2\left[(m_Y - m_p)^2 - m_K^2\right]}{4 m_p^2},$$

and g_Y is the $K^- pY$ coupling constant.

If the validity of the Pomeranchuk theorem[16] is assumed, then in the limit $W \to \infty$ the relation obtained by equating expressions (2) and (6) reduces to a conventional dispersion relation for $f_-(\omega)$ with one subtraction at the K^+p threshold energy. However, the validity of the finite energy relation which we obtain in this way for finite W is completely independent of the asymptotic behaviour of the scattering amplitude.

Let us suppose that the total cross sections are known experimentally in the range $m_K \leq \omega \leq W$, so that the integral $I(\omega)$ defined by eq. (3) is determined for all ω. We also assume for the moment that $J(\omega)$ is known, at least at intermediate energies ω (our method of determining this contribution is described in sect. 5). The term $D_+(m_K)$ may be evaluated in terms of the known K^+p scattering length. Thus, if $D_\pm(\omega)$ is known experimentally at some energy ω, then $\Delta(\mp\omega)$ is determined from eq. (2) in terms of experimental information, applying the crossing relation $D_-(-\omega) = D_+(\omega)$ in the case of K^+p scattering. Eq. (6), on the other hand, expresses $\Delta(\omega)$ as a sum of unknown contributions from the unphysical region. In analogy with the terminology introduced by Hamilton et al.[17] for a similar function, we refer to $\Delta(\omega)$ as the discrepancy function.

3. The Conformal Mapping Method

From eq. (6) it is clear that the discrepancy function $\Delta(\omega)$ has relatively little structure over most of the energy region $|\omega| > m_K$ in which it can be determined directly from experimental data. This is a consequence of the fact that $\Delta(\omega)$ at moderate or large values of $|\omega|$ is expressed as a sum of contributions from relatively distant energies. Therefore we may expect that $\Delta(\omega)$

can be well described in terms of a small number of parameters. The essence of our method is the fact that, by virtue of eq. (2), a fit to $\Delta(\omega)$ also constitutes a fit to $D_{\pm}(\omega)$. We obtain a rapidly convergent expansion for the discrepancy function by means of a variant of a conformal mapping technique which has been applied previously to various problems in high-energy physics and extensively discussed in the literature /18–24/.

It follows from eq. (6) that the only singularities of $\Delta(\omega)$ in the ω plane are two hyperon poles and the unphysical cut joining the branch points at $\omega_{\pi\Lambda}$ and m_K. We now introduce the new variable

$$\xi = \frac{\sqrt{\omega - m_K} - \sqrt{\omega - \omega_\Sigma}}{\sqrt{\omega - m_K} + \sqrt{\omega - \omega_\Sigma}}. \tag{7}$$

With an appropriate choice of the square roots, eq. (7) represents a conformal mapping $\xi(\omega)$ which transforms the entire cut ω plane into the unit circle $|\xi| = 1$ and its interior x/. In particular, the pole at $\omega = \omega_\Sigma$ is transformed to the point $\xi = 1$, the $K^- p$ threshold at $\omega = m_K$ to the point $\xi = -1$, and the unphysical cut for $\omega_{\pi\Lambda} \leq \omega \leq m_K$ to part of the unit circle. The region $m_K \leq \omega \leq \infty$ is mapped onto the interval $-1 \leq \xi \leq 0$, the region $-\infty \leq \omega \leq -m_K$ onto a small portion of the positive real axis, and the point $\omega = \omega_\Lambda$ onto a point on the real axis at $\xi = \xi_\Lambda \approx 0{,}36$. The point at infinity in the ω plane corresponds to $\xi = 0$. The resulting structure in the ξ plane is shown in fig. 1.

x/ The mapping which achieves this is not unique. A discussion of the reasons for the choice of the particular form (7) is deferred until sect. 8.

Thus, the discrepancy function $\Delta(\xi)$, regarded as a function of the new variable ξ , is analytic within the unit circle except for the pole at $\xi=\xi_\Lambda$. If this pole is removed explicitly, the resulting function may be expanded in a power series in the form

$$H(\xi)=(\xi-\xi_\Lambda)\Delta(\xi)=\sum_{n=0}^{\infty} a_n \xi^n, \tag{8}$$

convergent for all $|\xi|<1$. Our method is to determine as many coefficients of the expansion (8) as possible from the experimental knowledge of the discrepancy function.

4. Evaluation of the Discrepancy Function

We choose the cut-off energy W in eq. (3) to be 55 GeV. Numerical values of $I(\omega)$ are calculated in terms of the existing experimental data on $\sigma_\pm(\omega)$. References to the data up to 20 GeV can be found in ref.[7]. In addition, we use the Serpukhov data[8] on $\sigma_-(\omega)$ between 20 and 55 GeV.

Unfortunately, the K^+p total cross section has not been measured above 20 GeV. However, the data at lower energies indicate that $\sigma_+(\omega)$ is remarkably structureless and constant to within high accuracy from a few GeV up to 20 GeV, so that it seems relatively safe to extrapolate its constant value to higher energies. Thus, we assume that $\sigma_+(\omega)=(17.3\pm0.2)$ mb. between 20 and 55 GeV. Some of the recent fits to the $K^\pm p$ total cross sections, especially those including Regge cuts, predict a small rise in the value of $\sigma_+(\omega)$ within this energy range, typically up to 1 mb[9,10,12,13]. However, because of the rapid convergence of the integral $I(\omega)$, an error of this order of magnitude would not be serious; in fact, for the values of $|\omega|$ of the order of a few GeV at which the discrepancy function may be evaluated, such an error in the contribution to $I(\omega)$ from the region $\omega > 20$ GeV may be accurately compensated by an effective contribution to the high-energy integral $J(\omega)$, whose form we describe in terms of free parameters.

Since the $K^{\pm}p$ total cross sections have been measured less accurately at energies close to threshold, we make use of theoretical parametrization of the scattering data to calculate $\sigma_{\pm}(\omega)$ at low energies. For the integration over $\sigma_{+}(\omega)$ up to the kaon momentum $k = 664$ MeV/c, as well as the term $D_{+}(m_K)$ in eq. (2), we use the S-wave effective-range parameters determined from a recent analysis of $K^{+}p$ scattering at low energies [25]. For the integration over $\sigma_{-}(\omega)$ up to $k = 293$ MeV/c, we use the parameters determined from a recent S- and P-wave multichannel analysis of the low-energy $K^{-}p$ and $K_2^0 p$ data [26]. Other recent parametrizations of these data [27] give practically identical predictions for $\sigma_{-}(\omega)$ in the low-energy physical region but lead to rather different extrapolations of the amplitude into the unphysical region. For our purposes it is unimportant which parametrization is chosen, since our analysis does not require any information about the amplitude in the unphysical region.

Values of $|D_{\pm}(\omega)|$ may be obtained at many energies ω by comparing extrapolations of experimental $K^{\pm}p$ elastic differential cross sections to the forward direction with the corresponding optical limits determined from the total cross section data. For reasons discussed in the following section, we must avoid using values of the discrepancy function too close to the $K^{-}p$ elastic threshold or at energies which are too large in magnitude. We therefore confine our analysis to values of D_- at momenta k between 0.3 and 5 GeV/c and values of D_+ at $k < 5$ GeV/c. We have made an extensive search of the literature for experimental data on the angular distributions for $K^{\pm}p$ scattering in these momentum ranges. In this way we have determined the values of $|D_-|$ at 54 momenta from 0.35 to 4.6 GeV/c and $|D_+|$ at 35 momenta from 0.778 to 4.6 GeV/c[x]. As a rule, the signs of $D_{\pm}$ are undetermined experimentally, although at many energies they have been fixed unambiguously by means of dispersion relations[1-7]. Our procedure for fixing the remaining signs of $D_{\pm}$ in our calculations is defined in detail in sect. 6.

Reliable values of D_+ at low energies may be constructed with the aid of the effective range parameters for K^+p scattering. These parameters are now very well determined[25,27] and permit a significantly more accurate evaluation of D_+ than the individual fixed-energy measurements of K^+p scattering. We therefore supplement our set of 89 experimental data points for $|D_{\pm}|$ at higher momenta by 15 additional values of D_+ at equally-spaced energies in the momentum range $k < 0.55$ GeV/c, calculated by means of the same effective range parameters[25] which we use to evaluate the low-energy $\sigma_+(\omega)$ contribution to the integral $I(\omega)$. Thus, provided that the signs of $D_{\pm}$ and the values of $J(\omega)$ can be determined, the information summarized above leads to a knowledge of the discrepancy function $\Delta(\omega)$ at a total of 104 energies.

---

[x] Our complete compilation of the data on $|D_{\pm}|$, including some values which became available to us too late to be used in the present work, will appear elsewhere[28]. References to most of the data can be found in refs.[6,7,29].

5. The Parametrization

We truncate the power series (8) for the function $H(\xi)$, retaining only the first N coefficients $a_0, a_1, \dots, a_{N-1}$ as free parameters to be fitted to the values of the discrepancy function. The optimum value of N is determined by the usual statistical criteria. In addition, however, it is necessary to parametrize the unknown energy dependence of the high-energy contribution $J(\omega)$. We do this by expanding the integrand in the definition of $J(\omega)$, eq. (4), in powers of ω/ω'. Thus,

$$J(\omega) = \sum_{n=0}^{\infty} b_n \omega^n, \tag{9}$$

where

$$b_n = -\mathrm{Im} \int_{S(W)} \frac{f_-(\omega')\, d\omega'}{\omega'^{(n+1)} (\omega' + m_K)} \,. \tag{10}$$

The series (9) converges for all $|\omega| < W$. As additional parameters for the fit, we take the first M coefficients b_n of this series. From eq. (4) it is clear that the series (9) is rapidly convergent for $|\omega| \ll W$. In particular, $J(\omega) \approx J(0) = b_0$ for such energies. Thus, only a small number of terms is required if the analysis is restricted to energies sufficiently small in comparison with W.

To summarize our method, the procedure defined above amounts to a parametrization of the experimentally measurable function

$$G(\omega) = \Delta(\omega) - \frac{\omega + m_K}{\pi} J(\omega) \tag{11}$$

in the form

$$G(\omega) = \frac{1}{\xi - \xi_\Lambda} \sum_{n=0}^{\infty} a_n \xi^n - \frac{\omega + m_K}{\pi} \sum_{n=0}^{\infty} b_n \omega^n . \tag{12}$$

Although we have established the existence of this representation, it is worth while to point out that neither of the two series in eq. (12) would by itself be sufficient. This is a consequence of the analytic structure of $G(\omega)$ in the complex ω plane. From eqs. (4), (6) and (11) it can be seen that $G(\omega)$ has both the low-energy singularities (the hyperon poles and unphysical cut) and the high-energy cut (with branch points at $\omega = \pm W$). In the energy region of interest to us, a series of the first type in eq. (12) cannot represent $G(\omega)$ because of the high-energy singularities, while one of the second type cannot represent $G(\omega)$ because of the low-energy singularities.

To ensure rapid convergence of each of the series in eq. (12), it is necessary to impose certain restrictions on the range of values of ω over which the fit is made. Since the first series converges only within the unit circle in the ξ plane, we must exclude values of ω corresponding to $|\xi| \approx 1$, i.e. energies close to the K^-p elastic threshold. Similarly, since the second series converges only within the circle $|\omega| = W$, we must exclude values near this limit. These considerations account for the restrictions on the range of ω which were introduced in sect. 4.

6. Fit to the Real Parts

Our procedure is as follows. The function $G(\omega)$ defined above is known experimentally at various energies ω , except for an ambiguity due to the unknown signs of $D_\pm(\omega)$. We perform a least-squares fit to the values of $G(\omega)$ obtained by assuming a fixed set of signs for $D_{\pm}(\omega)$, in terms of a truncated expansion of the type (12) in which the N+M coefficients $a_0, \dots, a_{N-1}$, $b_0, \dots, b_{M-1}$ are treated as free parameters. Inverting eq. (2), we find in this way a fit to $D_{\pm}(\omega)$. The input and output signs of $D_{\pm}(\omega)$ are then compared at each energy. If any of the assumed input signs disagree with the corresponding output signs, these input signs are changed (leading automatically to an improved fit with the same parameter values) and a least-squares fit is found using the new values of $G(\omega)$. This procedure is iterated until all the corresponding input and output signs agree.

The entire sequence of operations is carried out under various initial assumptions about the signs of $D_{\pm}$ until it appears likely that a better final fit cannot be found. In this way we determine the set of signs for the $D_{\pm}$ data which leads to the best theoretical fit to the entire data set.

We have carried out the analysis for various numbers of parameters N and M in each of the two series. The first coefficient of the second series, b_0, was found to be accurately and consistently determined by the various fits and its inclusion was necessary for an acceptable fit. The inclusion of b_1, however, generally gave only a slight inprovement and its numerical value was less consistently determined by the various fits. Therefore we consider here in detail only those fits with $M = 1$.

Whenever any of the experimental data points for $D_{\pm}$ differed by more than five standard deviations from the corresponding final theoretical value from a particular fit, these points were rejected and the fit was repeated without them. Two particular data points were repeatedly rejected by this criterion, namely the values of

$|D_-|$ at 2.0 GeV/c [30] and $|D_+|$ at 1.455 GeV/c [31], both of which have rather small errors. The remaining experimental points were, as a rule, within 3.5 standard deviations from the theoretical predictions.

With $N = 1, 2, 3, 4, 5$ our best fits have values of χ^2 equal to 105, 101, 62, 60 and 60 respectively. The inclusion of further parameters does not give a substantial improvement and in fact leads to unreasonably large errors and correlation coefficients for the parameter values. We have therefore chosen $N = 4$ as the optimum value, corresponding to a 5-parameter fit. For our purposes the choice between the 4- and 5-parameter fits is unimportant, since their predictions for $D_\pm$ are practically identical within the entire energy range under consideration.

Since 102 values of $D_\pm$ are fitted, it may appear that χ^2 for our optimum fit is surprisingly small. This may be partly attributed to the fact that we constructed 15 values of D_+ from effective range theory. These values are certainly not statistically independent, so that the true number of degrees of freedom is somewhat smaller than the apparent number. Moreover, the two rejected points would have given rather large contribution to χ^2 if they had been retained in the fit.

Our predictions for $D_\pm$ and $\alpha_\pm \equiv D_\pm / A_\pm$ for the 5-parameter fit, for kaon momenta k between 0.5 and 3.0 GeV/c, are presented in table 1 in a form which may be compared directly with the tabulated results of the most recent analysis of Martin and Perrin [6]. We have restricted k to the range in which most of the interesting structure of $D_\pm$ occurs. This is also the momentum range in which most of the experimental data exist and in which our series expansions are most rapidly convergent. Over most of this range, the results for $a_{\pm}$ from the 4- and 5-parameter fits differ by less than 0.01.

Our predictions for D_+ over the entire momentum range are in excellent agreement with those tabulated in ref./6/ and the corresponding values of ϵ_+ are within 5% of each other. Our results for D_-, like all earlier predictions, show the expected local structures in the energy dependence of D_- which are associated with the resonance peaks in the K^-p total cross section. However, our values of D_- are on the whole, considerably more positive than those obtained from many of the earlier dispersion relation calculations/1-6/. In particular, we find that D_- remains positive for all $k > 0.55$ GeV/c, whereas some of the earlier calculations predicted further changes of sign in this region. Since there is little ambiguity in the experimental total cross section data, such differences can be accounted for within the framework of conventional dispersion relations only by changes in the assumptions about the hyperon pole terms and the amplitudes in the unphysical and asymptotic regions.

Even if we took the initial set of signs of $D_{\pm}$ from any of the earlier predictions, our procedure led to either a fit similar to the one shown in table 1 or a distinct fit with significantly larger χ^2. It is interesting to note, however, that we found a fit rather similar to that of Martin and Perrin/6/ if all the signs of $D_{\pm}$ were constrained to be identical with the signs predicted by them. We point out that we obtained the expected results in all cases in which certain information about $D_{\pm}$ is known unambiguously from forward dispersion relations/1-7/. In addition, we found an almost perfect fit to the accurately known values of $D_+(\omega)$ at low energies calcu- from effective range theory.

From a recent phase shift analysis of the low-energy K^+p scattering data it was found[32] that, in addition to the conventional solution which we have used, it is possible to construct a family of alternative solutions which are characterized by a positive sign for $D_+(\omega)$ at low energies. To investigate this point, we repeated the analysis without using any values of $D_+(\omega)$ in the low-energy region. Although the fit is less accurately determined in this case, it still requires $D_+(\omega) < 0$ at low energies and in fact favours values even more negative than for the conventional solution. We conclude that the K^+p scattering length is indeed negative and therefore we reject the alternative type of solution.

Discrepancies between the experimental values of D_- and dispersion relation predictions have often been noticed[2,4-6] in the momentum region below 2 GeV/c, where many of the earlier theoretical predictions were too small in magnitude. In ref.[6] such a discrepancy at momenta just below 0.9 GeV/c was attributed largely to an inappropriate choice of the number of terms of the Legendre polynomial series which was fitted to the K^-p angular distributions in ref.[33]. We find this explanation unconvincing, however, since, in contrast with many earlier calculations, we obtain a good fit to the entire data set. In fact, if we use the values of $|D_-|$ obtained in ref.[6] from a re-analysis of the experimental data of ref.[33], instead of the originally reported values, our best fit becomes somewhat poorer. Moreover, data on D_- from other independent experiments[34-36] near 0.9 GeV/c are in good agreement with the results of ref.[33] and with our fit.

7. Asymptotic Behaviour of the Scattering Amplitudes

The parameter b_0 in our fit characterizes the asymptotic behaviour of the scattering amplitudes. The value determined from the 5-parameter fit is

$$b_0 = (-3.4 \pm 0.6)\,\mathrm{GeV}^{-2}. \tag{13}$$

As a measure of the stability of this result, we may compare it with the value $b_0=(-3.6\pm0.2)$ GeV^{-2} obtained from the 4-parameter fit. The result (13) is of special interest, since any model for the asymptotic behaviour of the scattering amplitudes gives a definite prediction for this parameter.

By deforming the contour for the integration (10) into a path along the real axis for $|\omega| > W$ and a semicircle at infinity, and neglecting terms of order m_K/ω' in the integrand, we obtain

$$b_0 = -\frac{1}{4\pi}\int_W^{\infty}\frac{[\sigma_-(\omega')-\sigma_+(\omega')]\,d\omega'}{\omega'} \tag{14}$$

in the case in which the Pomeranchuk theorem is satisfied. According to the conventional Regge pole model, the $K^{\pm}p$ cross section difference may be parametrized at high energies in the form

$$\sigma_-(\omega)-\sigma_+(\omega) = 2\sum_i C_i\,(\omega/\omega_0)^{\alpha_i-1}, \tag{15}$$

where α_i are the trajectory intercepts, C_i are residue functions and ω_0 is some fixed scale factor; the summation is usually taken over the ρ and ω Regge poles. Substituting eq. (15) into (14), we obtain in this case

$$b_0 = \frac{1}{2\pi}\sum_i\frac{C_i\,(W/\omega_0)^{\alpha_i-1}}{\alpha_i-1}. \tag{16}$$

Next we consider models of the asymptotic behaviour which violate the Pomeranchuk theorem. If the $K^{\pm}p$ total cross sections tend to different asymptotic limits $\sigma_{\pm}(\infty)$, it follows from a twice-subtracted dispersion relation that the amplitudes have the asymptotic form[16]

$$f_{-}(\omega) = \frac{\omega\sigma_{-}(\infty)}{4\pi}\left[\frac{\sigma_{+}(\infty)-\sigma_{-}(\infty)}{\pi\sigma_{-}(\infty)}\log\left(\frac{\omega}{\omega_1}\right) - i\right], \tag{17}$$

where ω_1 is some constant.

Consider first the extreme assumption[15,37] that

$$\sigma_{\pm}(\omega) = \sigma_{\pm}(\infty) \qquad \text{for } |\omega| > W. \tag{18}$$

In this case it may by shown that the correct value of the contour integral (10) for the quantity b_0 is obtained if the asymptotic form (17) is used, even though this form is not necessarily locally correct on the contour of integration. The argument is as follows. The contour integral (10) may be deformed into the sum of an integration along the region $W<|\omega|<U$ of the real axis and an integration over a semicircle of radius U. Let U be sufficiently large that the integrand is given correctly on the semicircle in terms of the asymptotic form (17). This asymptotic form may also be used to evaluate the integral along the real axis, since this integral involves only $\mathrm{Im}\, f_{-}$, which is given correctly (to within terms of order m_K/ω) by eq. (17). Thus the analytic function (17) also leads to the correct result for the original contour. Substituting (17) into eq. (10), we find

$$b_0 = (4\pi)^{-1}[\sigma_{-}(\infty) - \sigma_{+}(\infty)]\log(W/\omega_1). \tag{19}$$

In more general models which violate the Pomeranchuk theorem, the amplitudes are described at high energies by a sum of conventional Regge pole terms and a term of the form (17). The expression for b_0 then becomes a sum of terms of the form (16) and (19).

In table 2 we present the predictions for b_0 from various phenomenological models for extrapolating the high-energy $K^{\pm}p$ scattering data to asymptotic energies. We also list the prediction for $\sigma_-(\infty)-\sigma_+(\infty)$ from each model to show the extent to which it violates the Pomeranchuk theorem. In several analyses only the total cross sections were parametrized directly, so that it was not clear what value to take for ω_1 in eq. (17). In these cases, however, the prediction for b_0 is not too sensitive to the value of ω_1 and for definiteness we set $\omega_1 = 1$ GeV.

As is obvious from eq. (14), models which satisfy the Pomeranchuk theorem and give the usual inequality $\sigma_-(\omega) > \sigma_+(\omega)$ predict $b_0<0$. However, we see from table 2 that all existing models of this type give values of b_0 several times smaller in magnitude than the result (13) obtained from our analysis. On the other hand, the component of the amplitude which violates the Pomeranchuk theorem gives a positive contribution to b_0, as is clear from eq. (19). This accounts for the positive values of b_0 for the last three models listed in table 2.

It may appear surprising that $b_0>0$ for such models, since in these cases the integrand of eq. (14) has the same sign as for models which satisfy the Pomeranchuk theorem but is even larger in magnitude. However, it must be remembered that the representation (14) breaks down in this case and must be replaced by a contour integral such as expression (10). It is easy to verify, in fact, that for the asymptotic form (17) the negative (divergent) integral (14) is completely compensated by a positive (divergent) value for the integral over the semicircular contour at infinity.

We conclude that our negative value of b_0 strongly favours a zero asymptotic limit $\sigma_-(\infty) - \sigma_+(\infty)$ but requires a considerably slower approach to this limit with increasing energy than that which is obtained from conventional Regge pole models.

8. Alternative Conformal Mappings

The conformal mapping (7), which tramsforms the interval $\omega_\Sigma \leq \omega \leq m_K$ onto the unit circle $|\xi| = 1$ and the remainder of the cut plane into the interior of this circle is not the only one having these properties. A one-parameter family of such mappings $\eta(\omega)$ may be constructed by applying the additional transformation

$$\eta = \frac{\xi - \lambda}{1 - \lambda\,\xi}, \tag{20}$$

where λ is a real parameter in the range $-1 < \lambda < 1$. This transformation maps the interior of the unit circle into itself, with $\xi = \pm 1$ as fixed points. It is characterized by the fact that the point at infinity in the ω plane is mapped into the point $\eta = -\lambda$ and the point $\xi = \lambda$ into the origin $\eta = 0$. Eq. (20) reduces to the identity transformation for the special case $\lambda = 0$ and $\eta(\omega)$ then becomes simply the mapping which we have already used. We now present an argument in favour of using this particular mapping.

Consider the expansion

$$H(\eta) = \sum_{n=0}^{\infty} a_n\, \eta^n \tag{21}$$

in analogy with eq. (3), where $H(\eta)=(\eta-\eta_{\Lambda})\Delta(\eta)$. It is well known that if $H(\eta)$ is an analytic function whose sungularities mearest to the origin lie on the unit circle $|\eta|=1$, then the terms of the expansion (21) for large n behave like $K\eta^{n}$, where K is some constant. In other words, the smaller the value of $|\eta|$, the more rapidly the series (21) converges, at least asymptotically. Hence it is desirable to use a transformation for which the region of energies over which the fit is made is concentrated as close as possible to the origin in the η plane, in order to reduce to a minimum the importance of the higher-order terms of the series. The comparison of the characteristics of various mappings given in table 3 shows that the one with $\lambda = 0$ is very close to the optimum according to this criterion.

As is evident from table 3, the geometric structure of the mapping $\eta(\omega)$ is very sensitive to the parameter λ. Therefore we obtain a strong consistency test by examining the stability of our results against small variations of this parameter. Repeating the 5-parameter fit for each of the two mappings defined by $\lambda = \pm 0.2$, we found that all the qualitative features of the fit described in sect. 6, such as the predicted signs of $D_{\pm}$, were perfectly reproduced and that the variation in the value of χ^{2} for the best fit was negligible. The numerical values found for $a_{\pm}$ in these cases differ from those shown in table 1 by less than 0.06 over most of the energy range considered. Moreover, the prediction for the parameter b_{0} varied from the value (13) by less than its statistical error. Thus, our results are quite stable under variations of the mapping.

Finally, we briefly discuss a class of possible alternative mappings $\eta(\omega)$ which could be used in connection with our method. One possibility is to map the larger interval of unphysical energies $\omega_\Lambda \leq \omega \leq m_K$ onto the unit circle, so that it becomes unnecessary to explicitly remove the Λ pole as in eq. (8). The appropriate mapping is obtained if the energy ω_Σ appearing in eq. (7) is replaced by ω_Λ. This mapping has two disadvantages, however. Firstly, we wish to study the possibility of analytically continuing the amplitude from the physical region to the Λ pole (see sect. 9). For this purpose the Λ pole must be mapped into a point in the interior of the circle. Secondly, the asymptotic convergence of the series representation for the discrepancy function is poorer in this case according to the criterion discussed above.

A second variant of the conformal mapping is one which transforms only the unphysical cut for $\omega_{\pi\Lambda} \leq \omega \leq m_K$ onto the unit circle. This corresponds to the replacement of ω_Σ by $\omega_{\pi\Lambda}$ in eq. (7). The Λ and Σ poles are then both mapped into the interior of the circle and it is necessary to add an additional factor $(\xi - \xi_\Sigma)$ in the definition of the function $H(\xi)$, eq. (8), in order to remove the Σ pole explicitly. The power series expansion in this case has the optimum rate of convergence according to the criterion given above. However, this criterion applies only to the behaviour of the terms of the series as $n \to \infty$. Because of the additional multiplicative factor $(\xi - \xi_\Sigma)$, the function which is fitted to the power series is likely to have more structure in the physical region than in the original case, so that a larger number of terms may be required for a good fit. In addition, there is a poorer separation of the Λ and Σ poles in this case, so that the possibility of continuing to the Λ pole appears less likely.

9. Continuation to the Λ Pole

Since our parametrization is based on series which converge at the Λ pole, it is possible in principle to use it to analytically continue the scattering amplitude from the physical region to this pole. In particular, from eq. (8) it follows that $H(\xi_\Lambda)$ is equal to the residue at the Λ pole in the variable ξ. Thus the corresponding residue $-X(\Lambda)$ in the variable ω, which is related in a simple way to the coupling constant g_Λ (see sect. 2), is given by

$$-X(\Lambda) = H(\xi_\Lambda)(d\omega/d\xi)_{\xi=\xi_\Lambda} . \tag{22}$$

From our 5-parameter fit we found in this way the value $g^2_\Lambda = 15\pm22$, which, within the errors, is consistent with all other recent determinations of this coupling constant [6,7,27]. However, it is important to note that the value of g^2_Λ, unlike the other predictions from our analysis which we have already discussed, is rather unstable with respect to variations of the number of parameters used in the fit as well as variations of the conformal mapping of the type described in the preceding section. We found that the variation in the value of g^2_Λ among the various acceptable fits is as large as ± 20. This suggest that, in addition to the purely statistical error for a given fit, there is an additional significant error in g^2_Λ due to the truncation of the power series (8). By considering the rate of convergence of this series, we shall now show that this is indeed the case.

In table 4 we give the numerical values of the individual terms $A_n(\xi) \equiv a_n\xi^n$ of the power series (8) for our standard 5-parameter fit ($N = 4$) at various values of ξ. Nearly all of the experimental $K^- p$ data which are used in the fit lie in the interval $-0.2 < \xi < 0$, while the entire $K^+ p$ physical region is contained in the interval $0 < \xi < 0.1$. From the numerical values of $A_n(\xi)$, it is clear that the convergence of the series is good over most of the region in which the data are fitted. However, the convergence is already quite poor at the position of the Λ pole, $\xi_\Lambda = 0.360$, where the terms A_2 and A_3 become comparable in magnitude. In fact, these two terms contribute there with opposite signs, so that the partial sum of the series for $N = 4$ is extremely sensitive to the point at which it is truncated. Thus, it would be necessary to determine more terms of the power series in order to obtain a reliable analytic continuation to the Λ pole. This is not possible using the experimental data which exist at the present time.

10. Alternative Parametrizations

We have already pointed out that the discrepancy function $\Delta(\omega)$ can be expressed as a sum of experimentally unknown contributions from the hyperon poles and the unphysical cut. This suggests that $\Delta(\omega)$ may be directly parametrized in terms of these unknown contributions.

In order to obtain an independent check of our results, we have also analyzed the experimental data by means of such parametrizations. In particular, the two hyperon pole terms in expression (6) for $\Delta(\omega)$ were replaced by a single effective pole term whose residue was taken as a free parameter. The amplitude on the unphysical cut was replaced by either a sum of one or two effective poles on the real axis, i.e., $A_{-}(\omega) = \Sigma\ B_n \delta(\omega - \omega_n)$ with B_n and ω_n (n = 1,2) as free parameters, or by a sum of one such pole and a Breit-Wigner resonance formula to represent the effect of the Y_0^* (1405) contribution. In addition, we allowed one or two free coefficients in the series (9) for the asymptotic contribution to the discrepancy function.

Only a small number of parameters could be determined from these fits. As expected, it was not possible to make an accurate determination of the separate contributions from the hyperon pole terms and the unphysical cut, since the values of the various parameters determined from the fits were highly correlated. Nevetherless, we obtained satisfactory fits to the experimental data on the real parts of the scattering amplitudes using various parametrizations of the types described above. Different parametrizations with approximately the same number of parameters led to similar fits.

The details of the resulting fits to the real parts, including the predicted signs, were all in excellent agreement with those obtained by the conformal mapping method. As before, we found that only the single high-energy parameter b_0 was required. The values of b_0 and their statistical errors obtained from the various fits were in excellent agreement with the previous result (13). The consistency of the results of this analysis with those of the conformal mapping method provides further confirmation of their stability and of the uniqueness of the fit.

In conclusion, we have obtained an accurate and reliable model-independent determination of the real parts of the $K^{\pm}p$ forward scattering amplitudes at moderate energies, as well as information about the asymptotic behaviour of the scattering amplitudes. However, the experimental data which are available at the present time do not permit a reliable analytic continuation of the scattering amplitude into the unphysical region.

One of us (N.M.Q) acknowledges with gratitude the kind hospitality of the Joint Institute for Nuclear Research and financial support from CERN. Discussions with Drs. W.N. Cottingham, V.A. Meshcheryakov and G. Violini have made significant contributions to this work. We also thank Ts. G. Istatkov for his help during the initial stages of this work.

References

1. N. Zovko. Z.Phys., 196, 16 (1966).
2. M. Lusignoli, M. Restignoli, G. Violini and G. A. Snow. Nuovo Cimento, 45A, 792 (1966); 46A, 430 (1966).
3. N.M. Queen. Nucl.Phys., B1, 207 (1967).
4. A.D. Martin and F. Poole. Nucl.Phys., B4, 467 (1968).
5. R. Levi-Setti. Proc. of the Lund Intern. Conf. on Elementary Particles (1969), p. 341.
6. A.D. Martin and R. Perrin. Nucl.Phys., B20, 287 (1970).
7. N.M. Queen, M. Restignoli and G. Violini. Fortschr.Phys., 17, 467 (1969).
8. J.V. Allaby et al. Phys.Letters, 30B, 500 (1969).
9. V. Barger and R.J.N. Phillips. Phys.Rev.Letters, 24, 291 (1970).
10. A.I. Lendel and K.A. Ter-Martirosyan. Pis'ma v ZhETF, 11, 70 (1969).
11. M. Restignoli and G. Violini. Phys.Letters, 31B, 533 (1970). Rome preprint n. 257.

12. J.C. Jackson. Arizona preprint ASU - HEP - 11 (1970).
13. V. Barger and R.J.N. Phillips. Phys.Letters. 31B, 643 (1970).
14. R. Arnowitt and P. Rotelli. Imperial College (London). Preprint ICTP/69/14.
15. O.V. Dumbrais and N.M. Queen. Phys.Letters, 32B, 65 (1970).
16. I.Ya. Pomeranchuk. ZhETF, 34, 725 (1958). English translation: Soviet Phys., JETP, 7, 499 (1958).
17. J. Hamilton, P. Menotti, G.C. Oades and L.L.J. Vick. Phys.Rev., 128, 1881 (1962).
18. W.R. Frazer. Phys.Rev., 123, 2180 (1961).
19. D. Atkinson. Phys.Rev., 128, 1908 (1962).
20. C. Lovelace. Nuovo Cimento, 25, 730 (1962).
21. S. Ciulli and J. Fischer. Nucl.Phys., 24, 465 (1961).
22. S. Ciulli and J. Fischer. ZhETF, 41, 256 (1961).
23. J.S. Levinger and R.F. Peierls. Phys.Rev., 134B, 1341 (1964).
24. J.E. Bowcock, W.N. Cottingham and J.G. Williams. Nucl. Phys., B3, 95 (1967).
25. A.D. Martin and R. Perrin. Nucl.Phys., B10, 125 (1969).
26. A.D. Martin and G.G. Ross. Nucl.Phys., B16, 479 (1970).
27. G. Ebel, H. Pilkuhn and F. Steiner. Nucl.Phys., B17, 1 (1970).
28. O.V. Dumbrais, T.Yu. Dumbrais and N.M. Queen JINR preprint, E 1-5259, Dubna (1970).
29. Particle Data Group, Berkeley preprint UCRL-20000 (1969).
30. R. Crittenden et al. Phys.Rev.Letters, 12, 429 (1964).
31. A. Bettini et al. Phys.Letters, 16, 83 (1965).
32. B. Carreras, A. Donnachie and R.G. Kirsopp. Daresbury preprint (1970).
33. B. Conforto et al. Nucl.Phys., B8, 265 (1968).
34. P.L. Bastien and J.P. Berge. Phys.Rev.Letters, 10, 188 (1963).

35. L. Bertanza et al. Phys.Rev., <u>177</u>, 2036 (1969).
36. R. Armenteros et al. preprint CERN/D.Ph.II/Phys. 70-7.
37. D. Horn. Phys.Letters, <u>31B</u>, 30 (1970).
38. R.J.N. Phillips and W. Rarita. Phys.Rev., <u>139B</u>, 1336 (1965).
39. G.V. Dass, C. Michael and R.J.N. Phillips. Nucl.Phys., <u>B9</u>, 549 (1969).

Received by Publishing Department
on July, 2, 1970.

Table 1

The predicted real parts $D_\pm$ and the ratios $\alpha_\pm \equiv D_\pm / A_\pm$. A typical error for $\alpha_\pm$ is ± 0.02.

k (GeV/c)	D_+ (GeV^{-1})	α_+	D_- (GeV^{-1})	α_-
0.5	-2.39	-I.86	-0.90	-0.I8
0.6	-2.33	-I.53	I.I2	0.28
0.7	-2.I9	-I.35	3.07	0.62
0.8	-2.05	-I.0I	4.I8	0.63
0.9	-I.92	-0.74	4.80	0.60
I.0	-I.93	-0.60	4.3I	0.42
I.I	-2.05	-0.53	I.68	0.I6
I.2	-2.46	-0.54	I.86	0.2I
I.3	-2.82	-0.57	2.73	0.32
I.4	-3.2I	-0.6I	3.26	0.36
I.5	-3.45	-0.63	3.46	0.34
I.6	-3.66	-0.63	3.48	0.3I
I.7	-3.88	-0.63	3.50	0.30
I.8	-4.I0	-0.63	3.52	0.30
I.9	-4.32	-0.63	3.54	0.30
2.0	-4.54	-0.63	3.62	0.29
2.I	-4.74	-0.63	3.76	0.29
2.2	-4.93	-0.62	3.89	0.29
2.3	-5.I2	-0.62	3.97	0.28
2.4	-5.33	-0.62	4.0I	0.28
2.5	-5.55	-0.62	4.05	0.28
2.6	-5.76	-0.62	4.09	0.27
2.7	-5.96	-0.62	4.I4	0.27
2.8	-6.I8	-0.62	4.20	0.26
2.9	-6.39	-0.62	4.25	0.26
3.0	-6.58	-0.62	4.3I	0.26

TABLE 2

The predictions for the parameter b_o from various models for the high-energy behaviour and the corresponding values for the asymptotic cross section difference.

Reference and model	$\sigma_-(\infty) - \sigma_+(\infty)$ (mb)	b_o (GeV^{-2})
Phillips and Rarita [38] Solution 1	0	-1.0
Dass et al. [39] Models (a), (i)	0	-0.7
Barger and Phillips [9]	0	-0.7
Restignoli and Violini [11] Solution IIa	0	-1.3
Jackson [12] Model without constraints	0	-1.2
Barger and Phillips [13]	2.5	1.5
Arnowitt and Rotelli [14]	2.1$\pm$0.3	1.4$\pm$0.3
Dumbrais and Queen [15]	3.7$\pm$0.5	3.0$\pm$0.4

TABLE 3

Values of η corresponding to various energies ω, as a function of the parameter λ in the mapping defined by eqs. (7) and (20).

λ	1 GeV	2 GeV	$\pm\infty$	-2 GeV	-1 GeV	ω_Λ
-0.2	0.07	0.15	0.20	0.23	0.26	0.52
0.0	-0.13	-0.05	0.00	0.04	0.06	0.36
0.2	-0.32	-0.25	-0.20	-0.17	-0.14	0.17

TABLE 4

Values (in fm units) of the individual terms $A_n \equiv a_n \xi^n$ of the power series (8) for the 5-parameter fit (N=4) at various values of ξ.

ξ	A_o	A_1	A_2	A_3
± 0.05	0.059	± 0.007	0.016	∓ 0.002
± 0.10	0.059	± 0.014	0.064	∓ 0.013
± 0.20	0.059	± 0.027	0.256	∓ 0.106
± 0.36	0.059	± 0.049	0.830	∓ 0.618

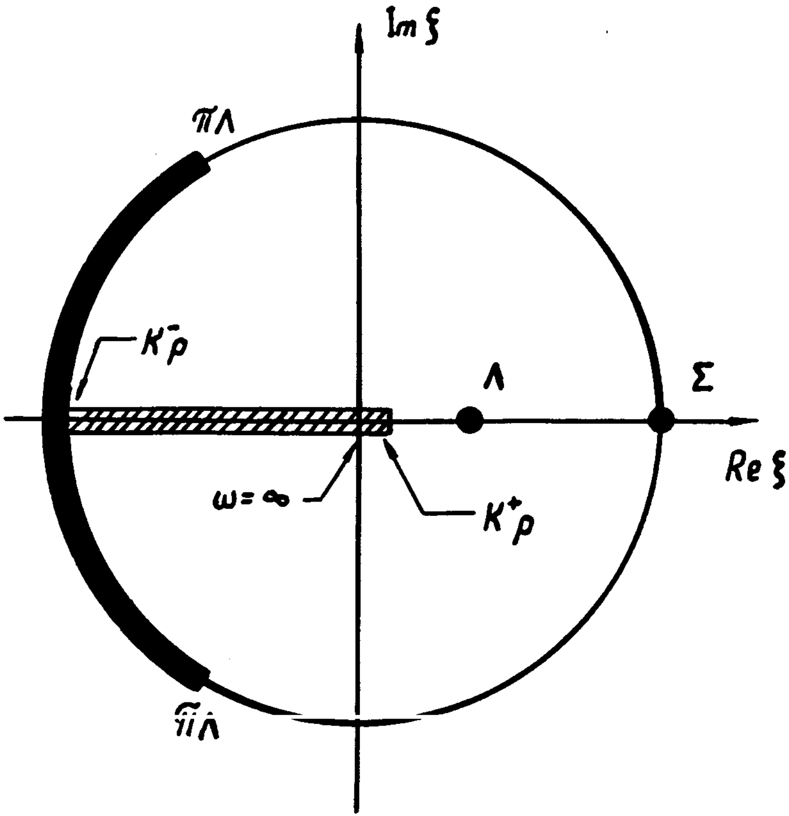

Fig. 1. The structure of the discrepancy function in the ξ plane. The black circles and lines show the poles and cuts. The physical region is indicated by the shaded area along the real axis.